COPY NO. 86

TECHNICAL REPORT 4152

FAILURE OF ADHESIVE BONDS AT CONSTANT STRAIN RATES

BY
ELISE McABEE
MICHAEL J. BODNAR
WILLIAM C. TANNER
DAVID W. LEVI

MARCH 1971

PICATINNY ARSENAL
DOVER, NEW JERSEY

The findings in this report are not to be construed as an official Department of the Army position.

DISPOSITION

Destroy this report when no longer needed. Do not return to the originator.

Technical Report 4152

FAILURE OF ADHESIVE BONDS AT CONSTANT STRAIN RATES

by

Elise McAbee
Michael J. Bodnar
William C. Tanner
David W. Levi

March 1971

AMCMS Code 4010.28.9.02003

Materials Engineering Laboratory
Feltman Research Laboratories
Picatinny Arsenal
Dover, N. J.

ACKNOWLEDGMENTS

The constant stress data was provided by Mr. R. F. Wegman. Thanks are also due Mrs. Dorothy Teetsel for assistance with the manuscript.

TABLE OF CONTENTS

Figures

OBJECT

The object of this work was to study the shear strength of a structural ahesive used in Army helicopters as a function of strain rate and failure time at several temperatures.

SUMMARY

Shear strengths of adhesive AF126 bonds to two thicknesses of aluminum were measured at constant rate of crosshead separation. Primarily cohesive failure was observed in all cases. By using relations proposed by Cherry and Holmes, the shear strength could be quantitatively related to temperature and strain rate or failure time. Of specific engineering interest would be the possibility of determining the reliability of a bonded joint for specific periods of time as a function of continuously applied stress at a given temperature.

INTRODUCTION

Scientists in the Materials Engineering Laboratory at Picatinny Arsenal have in the past shown some interest in the causes of failure of adhesive bonds under various loading conditions (Refs 1, 2). More recently, some constant strain rate shear strength determinations have been made on an AF126 adhesive used for structural bonding in Army helicopters. This paper shows that the shear strength of such a bond, under conditions where cohesive failure occurs, can be quantitatively related to temperature and strain rate or failure time.

RESULTS AND DISCUSSION

Tables 1 and 2 show the data for the constant strain rate (constant crosshead separation) measurements on 1/8 inch and 1/16 inch aluminum adherends bonded with AF126 adhesive. Three crosshead rates (0.105, 0.8, and 2 in. per min) were used at each of six temperatures (193^{o}, 233^{o}, 273^{o}, 296^{o}, 323^{o}, and 343^{o}K).

Cherry and Holmes (Ref 3) suggested that when a shear stress is applied to a polymer there is an instantaneous elastic deformation resulting from bond angle bending as well as simultaneous plastic deformation, stretching the polymer chains joining adjacent slipped

areas of the polymer until these chains break. When a critical rate of chain scission is exceeded, catastrophic failure occurs. For constant strain rate experiments, they obtained the relation

$$S = (2kT/\beta)\ln C + (2kT/\beta)\ln(hl/\rho\beta RT) + (2RG_e)^{1/2} + 2\varepsilon_o/\beta \quad (1)$$

S is stress at failure, β is volume of elements that respond in failure, C is rate of crosshead separation, ℓ is diameter of "dislocation loop", ρ is density of dislocation lines in unit volume of the medium $(2RG_e)^{1/2}$ is a critical value of strain at failure, and ε_o is an activation energy barrier. Since the last three terms on the right-hand side of Equation 1 are constant at a given temperature, this equation requires that a plot of S versus log C be linear. Figures 1 and 2 show such plots for the data given in Tables 1 and 2.

An alternative form of Equation 1 may be obtained by dividing through by T

$$S/T = (2k/\beta)\ln C + \frac{2k}{\beta}\ln\left(\frac{hl}{\rho\beta RT}\right) + \frac{(2RG_e)^{1/2}}{T} + \frac{2\varepsilon_o}{\beta T} \quad (2)$$

In this case, the S/T vs log C plots should be linear for each temperature. Figures 3 and 4 show the appropriate straight lines.

Equations 1 and 2 suggest that S or S/T should also be linear with log $(1/t_f)$. This will be so if the deformation (ε) is constant at a given temperature. (t_f is failure time.)

$$Ct_f = \varepsilon \quad (3)$$

The Ct_f products shown in Table 3 give an indication of the constancy of ε at each temperature. For 1/16 inch aluminum in the three cases where values are not recorded, the machine stalled on release, leading to a hesitation and longer times than would otherwise have been observed. A somewhat more convenient representation can be given by rearranging Equation 3 and taking logarithms.

$$\log C = \log \varepsilon + \log (1/t_f) \quad (4)$$

Equation 4 shows that a plot of log C versus log $(1/t_f)$ drawn with a slope = 1 will yield ε at log $(1/t_f) = 0$. Figures 5 and 6 show the straight lines drawn with slope = 1 in each case. Values of log ε obtained from these lines are given in Table 4.

It is interesting to note that there appears to be a small but noticeable variation of deformation with temperature for the samples using 1/8 inch aluminum adherends. In the case of 1/16 inch aluminum adherends, the deformation does not appear to vary with temperature, at least beyond the range of experimental error. The deformation (as used in this report and calculated from the observed C and t_f values) is presumably made up of grip slippage, and deformation in the links of the machine, the aluminum metal adherends, and the adhesive. The 1/16 inch aluminum adherends deform visibly under the test conditions while the 1/8 inch aluminum adherends do not. The observed differences are probably due to this difference in the response of the aluminum.

The reasonable constancy of the deformation at a given temperature for each of the crosshead rates makes it possible to replace log C in either Equation 1 or Equation 2 with log ε + log $(1/t_f)$. Then at a given temperature S(or S/T) should be linear with log $(1/t_f)$.

$$S = \frac{(2kT)}{\beta} \ln\varepsilon + \frac{(2kT)}{\beta} \ln\frac{(1)}{t_f} + \frac{2kT}{\beta} \ln\frac{(h1)}{\rho\beta kT} + (2RG_e)^{1/2} + \frac{2\varepsilon_o}{\beta} \qquad (5)$$

or

$$\frac{S}{T} = \frac{(2k)}{\beta} \ln\varepsilon + \frac{(2k)}{\beta} \ln\frac{(1)}{t_f} + \frac{2k}{\beta} \ln\frac{(h1)}{\rho\beta kT} + \frac{(2RG)^{1/2}}{T} + \frac{2\varepsilon_o}{\beta T} \qquad (6)$$

Figures 7-10 show that the lines required by Equations 5 and 6 are reasonably linear.

Equations 1, 2, 5, and 6 clearly indicate that the slopes of the lines in Figures 1-4, and 7-10 permit evaluation of β. Table 5 gives values of β determined from each of the four plots at each thickness of aluminum adherend. Average values are summarized in Table 6. Although numerical values of β for the crosslinked modified epoxy are considerably lower than those found by Cherry and Holmes (Ref 3) for polyethylene, β increases with temperature as observed by those investigators.

Some constant stress data for AF126 adhesive used with 1/16 inch aluminum panels is available (Ref 2). In this case, Cherry and Holmes (Ref 3) obtained the relation

$$S = \frac{(-2kT)}{\beta} \ln t_f + \frac{(2kT)}{\beta} \ln \frac{(h \dot{\gamma}_f)}{\rho \beta kT} + (2RG_e)^{1/2} + 2\varepsilon_o/\beta \qquad (7)$$

Equation 7 requires that S be linear with log t_f with β readily accessible from the slope as in the case of constant rate of strain experiments. Such a comparison should be useful in giving an indication that the same parameters describe the behavior under differing types of loading. Unfortunately, a direct comparison is not possible since at the long times of the constant stress experiments, the failure time was rather markedly dependent on humidity (Ref 2). Also, at the much lower loads of the constant stress experiments, there was no noticeable deformation of the 1/16 inch aluminum. Hence, a quantitative comparison of β values for the two cases does not seem to be in order. However, Figures 11-13 show that the constant stress data, allowing for the expected adhesive scatter, does obey Equation 7. This gives some confidence that these relations can describe data obtained by different loading methods. Table 7 gives apparent β values calculated from the slopes of the lines in Figures 11-13. Qualitatively, the values appear to be in the general range that would be expected from the results described above. However, in each case, there seems to be a rather sharp and unexpected downturn in the β (increase in slope) curve at the highest temperature (344°K).

EXPERIMENTAL PROCEDURE

Materials

2024-T3 aluminum panels, 4" x 13" x 1/8".

2024-T3 aluminum panels, 4" x 12" x 1/16".

AF126-3, a thermosetting, nonvolatile, modified epoxy film adhesive designed for structural bonding of metals.

Preparation of Adherends

Scribe marks were placed 1/2 inch from the long edge of each panel to assure an accurate overlap of the joint. Two panels were then clamped together in the position for bonding using the scribe marks as a guide. Alignment holes were drilled through the area to be bonded at both ends of the panel. The clamps were then removed and the panels were washed with acetone followed by degreasing in hot vapors of stabilized perchloroethylene. The area to be bonded was then etched for 5 minutes at 150°F in FPL etch solution in accordance with MIL-A-9067C, washed with tap water at 140°F, and rinsed in deionized water. The panels were dried in a forced-air circulating oven at 140°F for one hour.

Preparation of Lap Shear Specimens

One group of panels was prepared using the 1/16 inch thick aluminum adherends and a second group was prepared using the 1/8 inch thick adherends.

A single layer of the film adhesive was placed in the joint and the two adherend panels were pinned in place by putting aluminum rods through the previously drilled holes and hammering the protruding ends flat. Three bonded panels were prepared at one time, overlapping the ends to give them proper support. An extra panel was used for the same purpose under the end of the third bonded panel. The assembly was placed in a hydraulic press at room temperature and subjected to 50 psi pressure. The temperature was raised to 250°F at a rate of approximately 8°F per minute. The pressure and temperature were maintained for one hour. The assembly was then cooled under pressure. These conditions produced a glue line thickness of 2-3 mils. One-inch-wide specimens were cut from the panels with a bandsaw. The pieces from the ends of each panel were discarded.

Specimen Testing

The testing temperatures were maintained by using liquid carbon dioxide and electric heaters as required with a Standard test cabinet. The load was applied with a 60,000-pound Baldwin testing machine operating at a constant rate of crosshead separation. Failure times were measured with a stop watch.

REFERENCES

1. E. McAbee, W. C. Tanner and D. W. Levi, J. Adhesion 2, 106(1970)

2. E. McAbee and D. W. Levi, Prediction of Failure Times of Adhesive Bonds at Constant Stress, PATR 4105, in press.

3. B. W. Cherry and C. M. Holmes, Brit. J. Appl. Phys. (J. Phys. D) 2(2), 821 (1969)

TABLE 1

Failure data for AF126 adhesive with 1/8 inch thick aluminum adherends at constant strain rate

Temperature, °K	Crosshead Separation Rate (C), in./min	S, psi	S/T	t_f, min
193	0.105	6100	31.6	1.608
193	0.8	5330	27.6	0.203
193	2	4540	23.5	0.0805
233	0.105	6310	27.1	1.423
233	0.8	5920	25.4	0.198
233	2	5020	21.5	0.065
273	0.105	6300	23.1	1.508
273	0.8	6060	22.2	0.195
273	2	5050	18.5	0.065
296	0.105	5740	19.4	1.332
296	0.8	5490	18.5	0.190
296	2	4870	16.4	0.060
323	0.105	4860	15.1	1.200
323	0.8	4610	14.3	0.160
323	2	4120	12.8	0.053
343	0.105	3790	11.0	1.140
343	0.8	3920	11.4	0.152
343	2	3540	10.3	0.053

TABLE 2

Failure data for AF126 adhesive with 1/16 inch aluminum adherends at constant strain rate

Temperature, °K	Crosshead Separation Rate (C), in./min	S, psi	S/T	t_f, min
193	0.105	4760	24.7	1.470
193	0.8	4510	23.4	1.428
193	2	4300	22.3	0.108
233	0.105	5410	23.2	1.735
233	0.8	5280	22.7	0.265
233	2	4800	20.6	0.093
273	0.105	5300	19.4	1.657
273	0.8	5160	18.9	0.250
273	2	4660	17.1	0.097
296	0.105	4880	16.5	2.165
296	0.8	4870	16.5	1.747
296	2	4430	14.9	0.108
323	0.105	4320	13.4	1.538
323	0.8	4280	13.3	0.222
323	2	3810	11.8	0.092
343	0.105	2790	8.1	1.893
343	0.8	2520	7.3	0.793
343	2	2750	8.0	0.085

TABLE 3

Deformation from C and t_f values

Temperature, °K	C	$\varepsilon = C\, t_f$ 1/8 inch Al	1/16 inch Al
193	0.105	0.17	0.15
193	0.8	0.16	----
193	2	0.17	0.22
233	0.105	0.15	0.18
233	0.8	0.16	0.21
233	2	0.13	0.19
273	0.105	0.16	0.17
273	0.8	0.20	0.20
273	2	0.13	0.19
296	0.105	0.14	0.23
296	0.8	0.15	----
296	2	0.12	0.22
323	0.105	0.13	0.16
323	0.8	0.13	0.18
323	2	0.11	0.18
343	0.105	0.12	0.20
343	0.8	0.12	----
343	2	0.11	0.17

TABLE 4

Deformation from log C versus log ($1/t_f$) plots

Temperature, °K	log ε	
	1/8 inch Aluminum	1/16 inch Aluminum
193	-0.77	-0.74
233	-0.86	-0.71
273	-0.86	-0.70
296	-0.88	-0.65
323	-0.95	-0.73
343	-0.96	-0.70

TABLE 5

β Values from slopes of the various plots

Temperature, °K	β, Å^3 1/8 inch Aluminum	1/16 inch Aluminum
	From S Versus Log C Plots	
193	1470	5150
233	2350	4920
273	2880	5610
296	4350	9250
323	5520	8600
343	7790	10400
	From S/T Versus Log C Plots	
193	1480	5150
233	2350	5150
273	3020	5660
296	4230	8650
323	5770	8650
343	9070	11300
	From S Versus Log $(1/t_f)$ Plots	
193	1510	4370
233	2350	4690
273	3010	5270
296	4260	7660
323	5860	7910
343	8900	10400
	From S/T Versus Log $(1/t_f)$ Plots	
193	1480	4120
233	2350	4780
273	2890	5040
296	4230	7570
323	5290	6760
343	9070	11300

TABLE 6

Variation of average β values with temperature

Temperature, °K	β, A°3	
	1/8 inch Aluminum	1/16 inch Aluminum
193	1500	4700
233	2350	4900
273	2950	5400
296	4300	8300
323	5600	8000
343	8700	11000

TABLE 7

β Values derived from constant stress data

Temperature, °K	β, A°3		
	20% RH	50% RH	95% RH
296	----	----	3800
322	8100	9700	5500
333	9100	10000	7000
344	5200	7800	5900

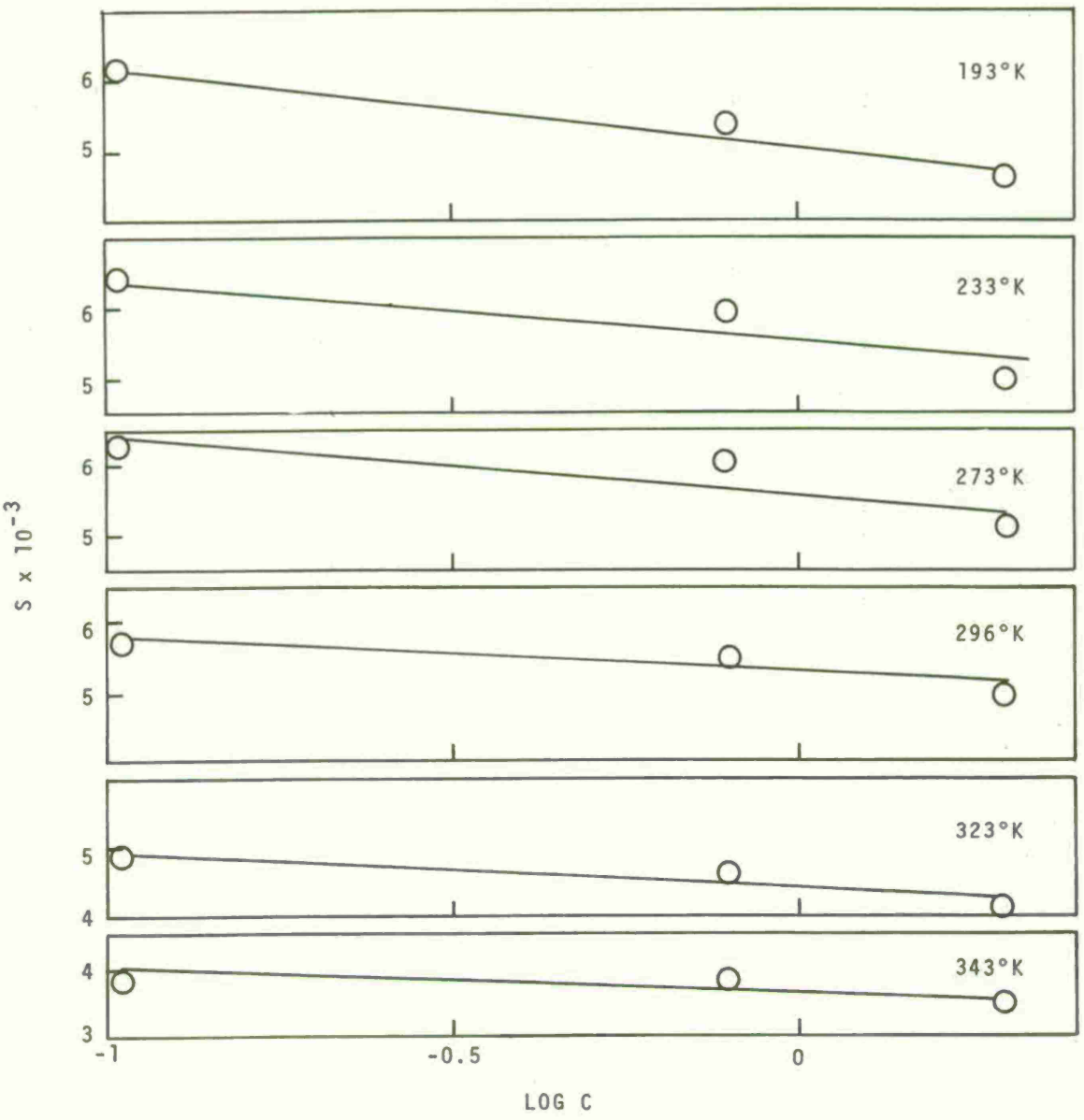

Fig 1 S versus log C for AF126 adhesive with 1/8" aluminum adherends

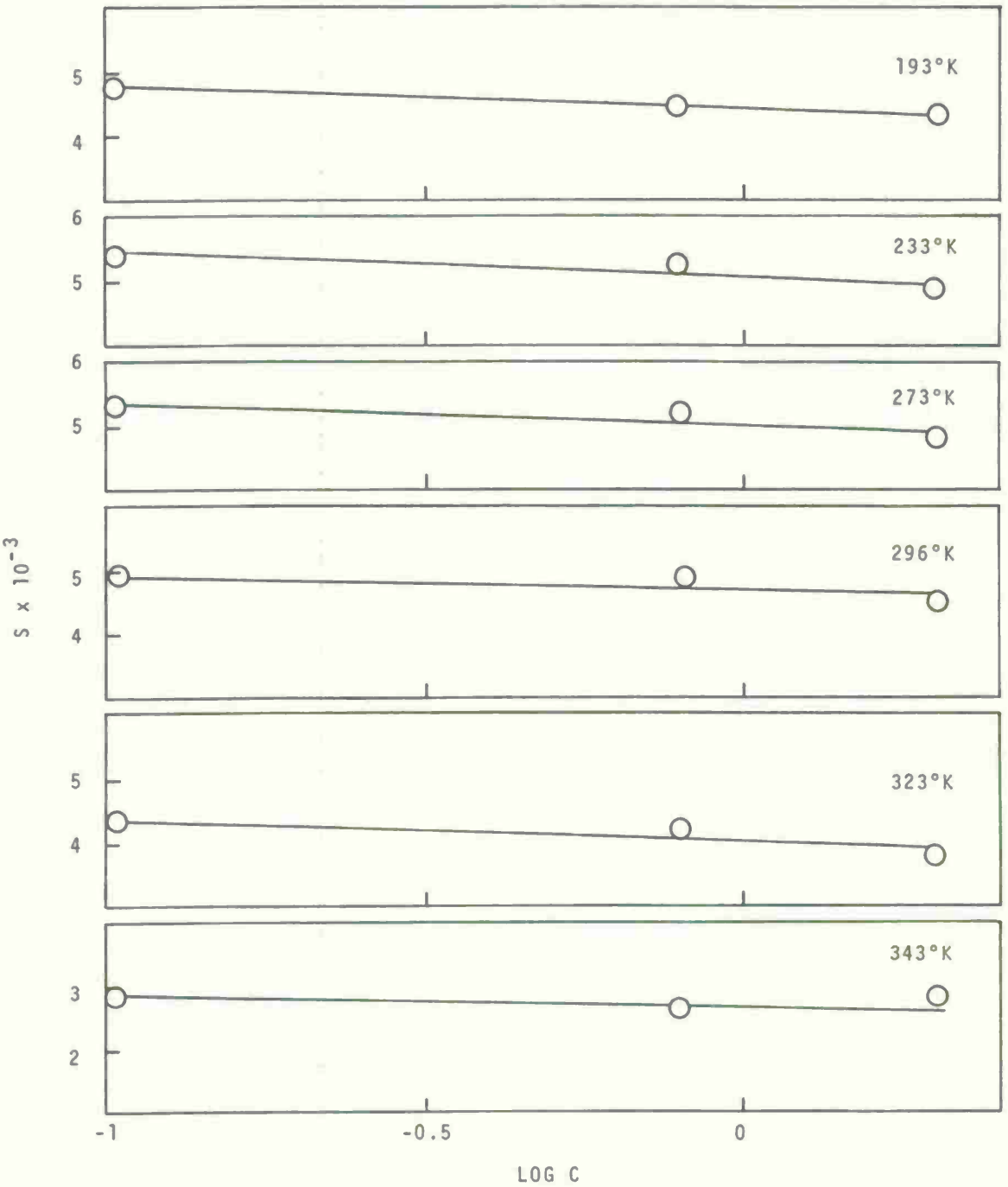

Fig 2 S versus log C for AF126 adhesive with 1/16" aluminum adherends

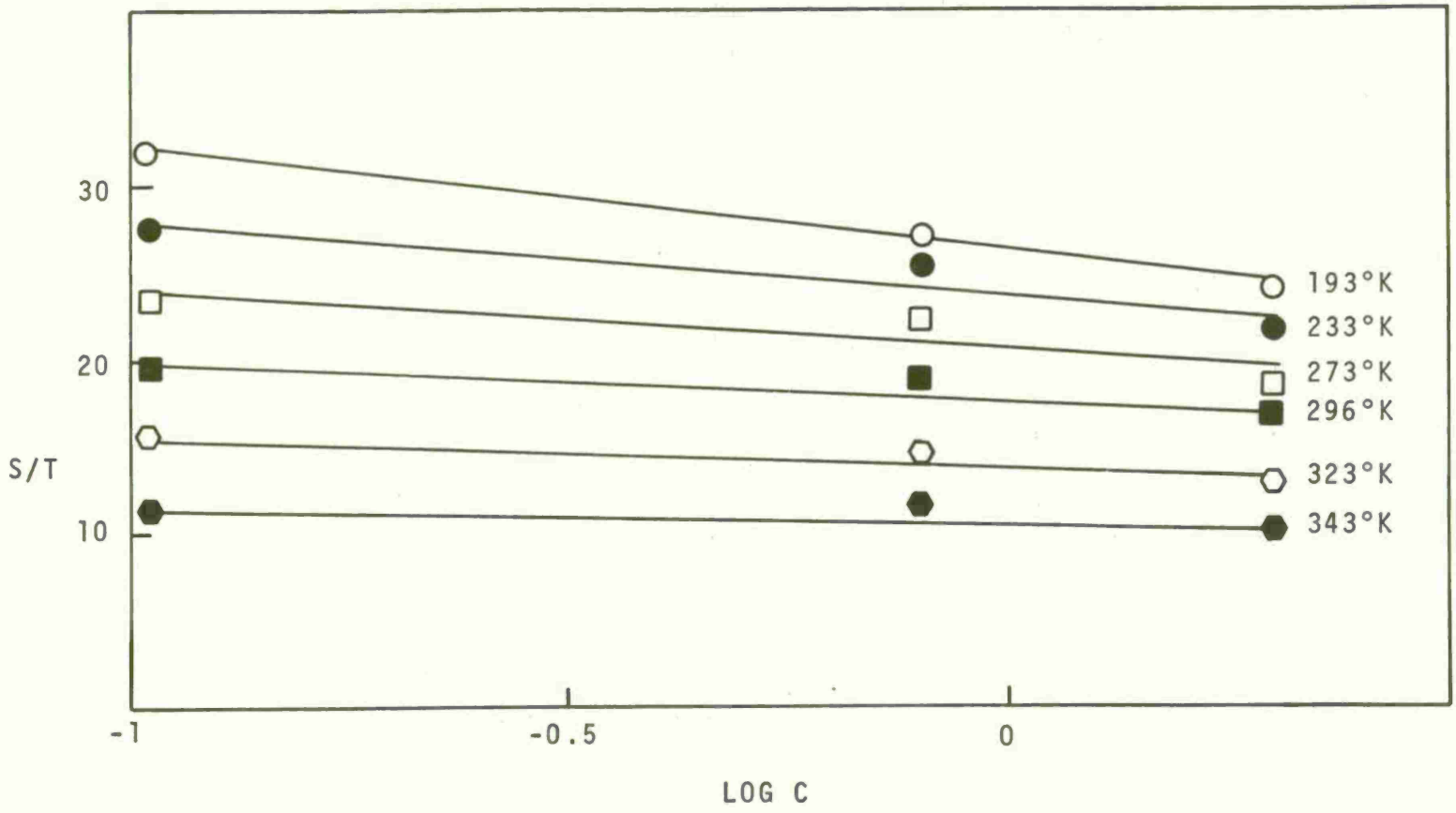

Fig 3 S/T versus log C for AF126 adhesive with 1/8" aluminum adherends

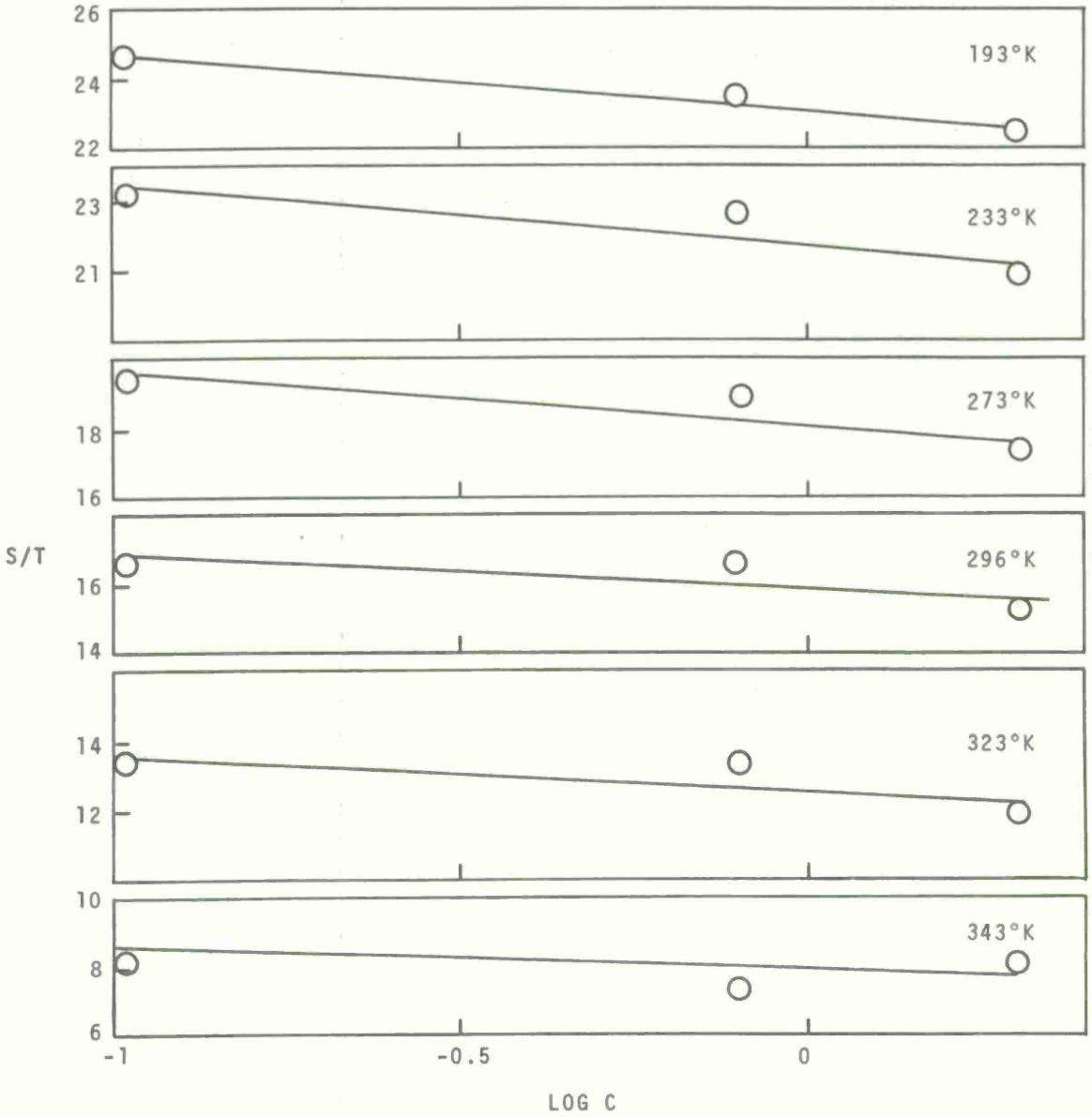

Fig 4 S/T versus log C for AF126 adhesive with 1/16" aluminum adherends

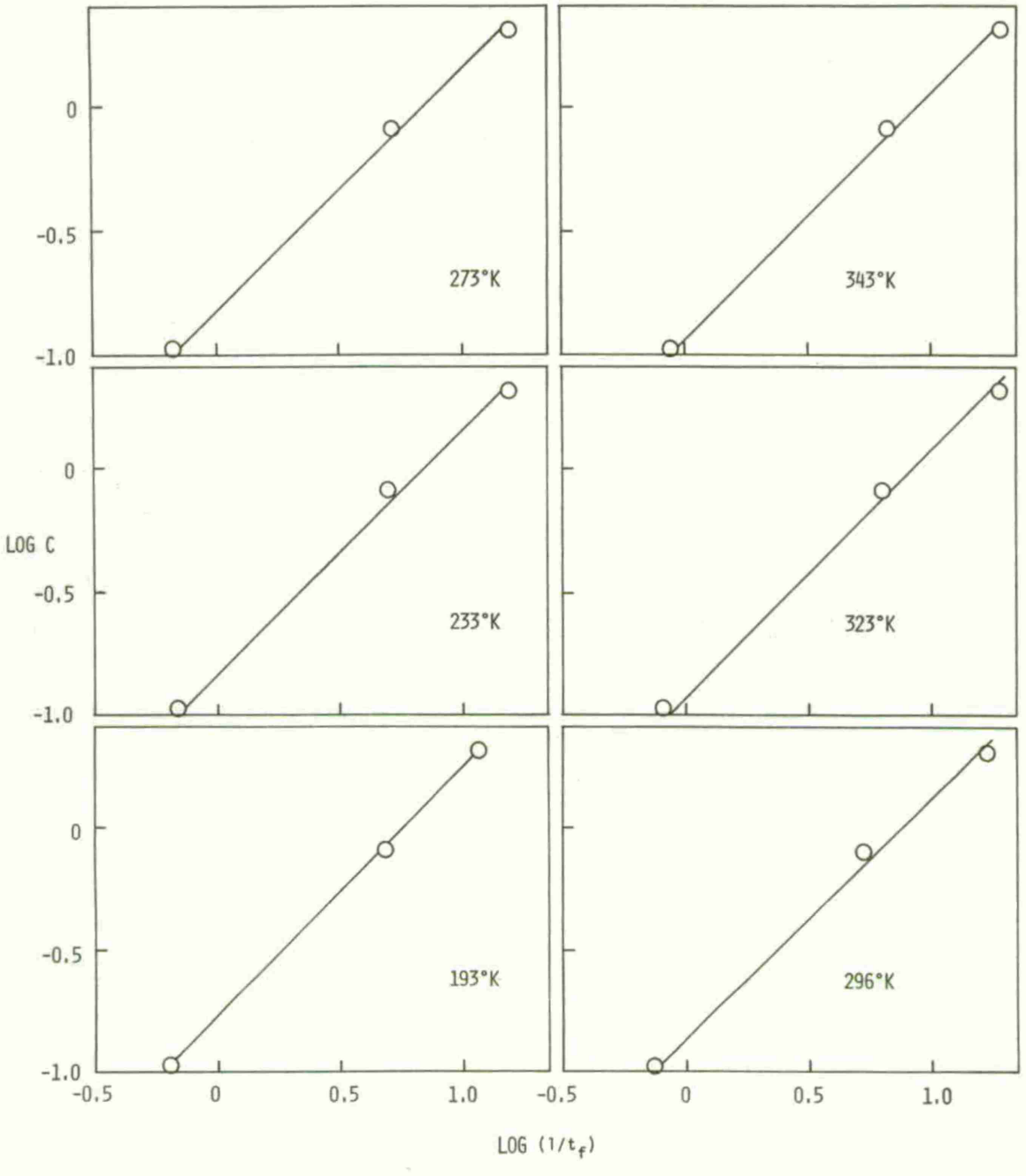

Fig 5 Log C versus log ($1/t_f$) for AF126 adhesives with 1/8" aluminum adherends

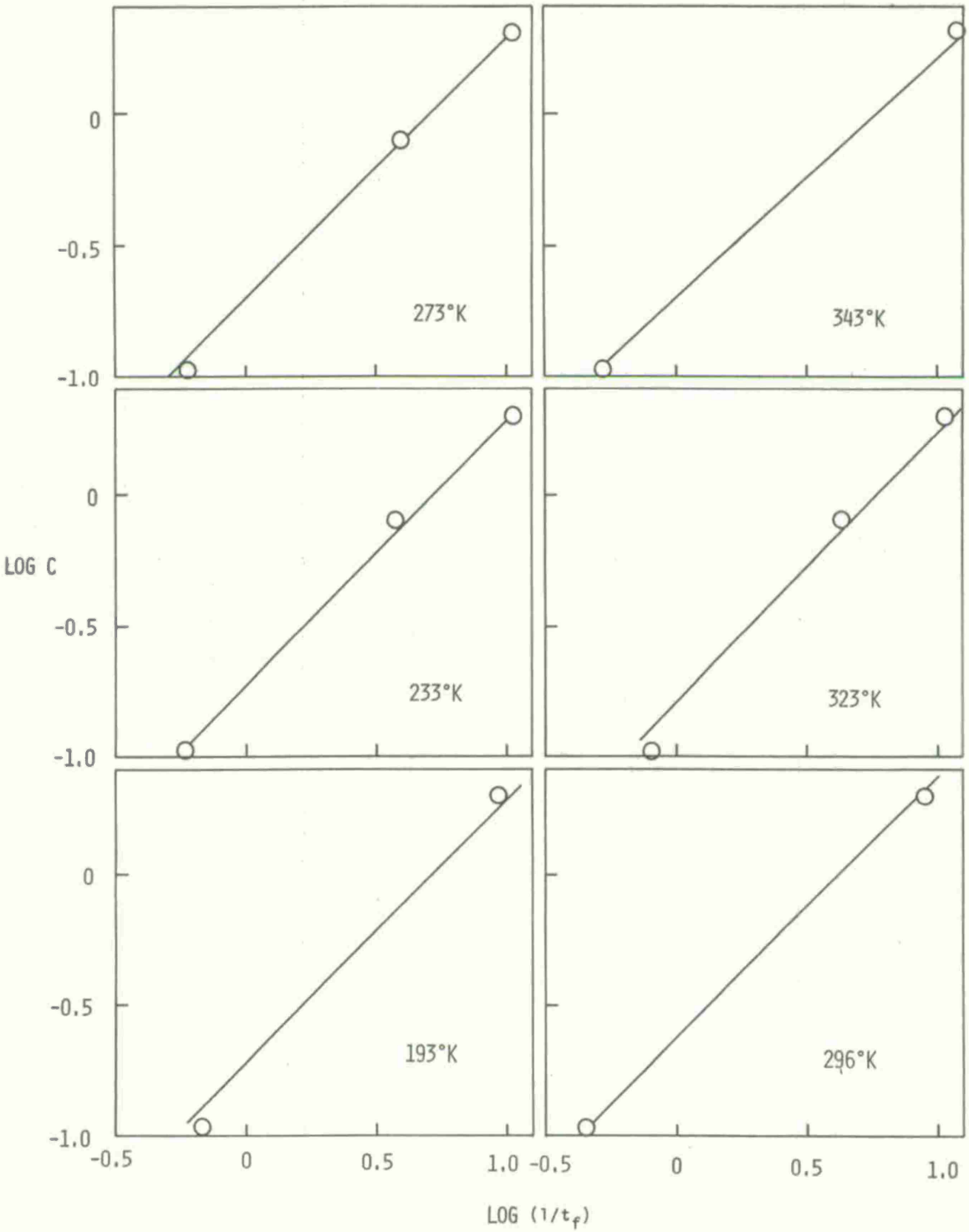

Fig 6 Log C versus log ($1/t_f$) for AF126 adhesive with 1/16" aluminum adherends

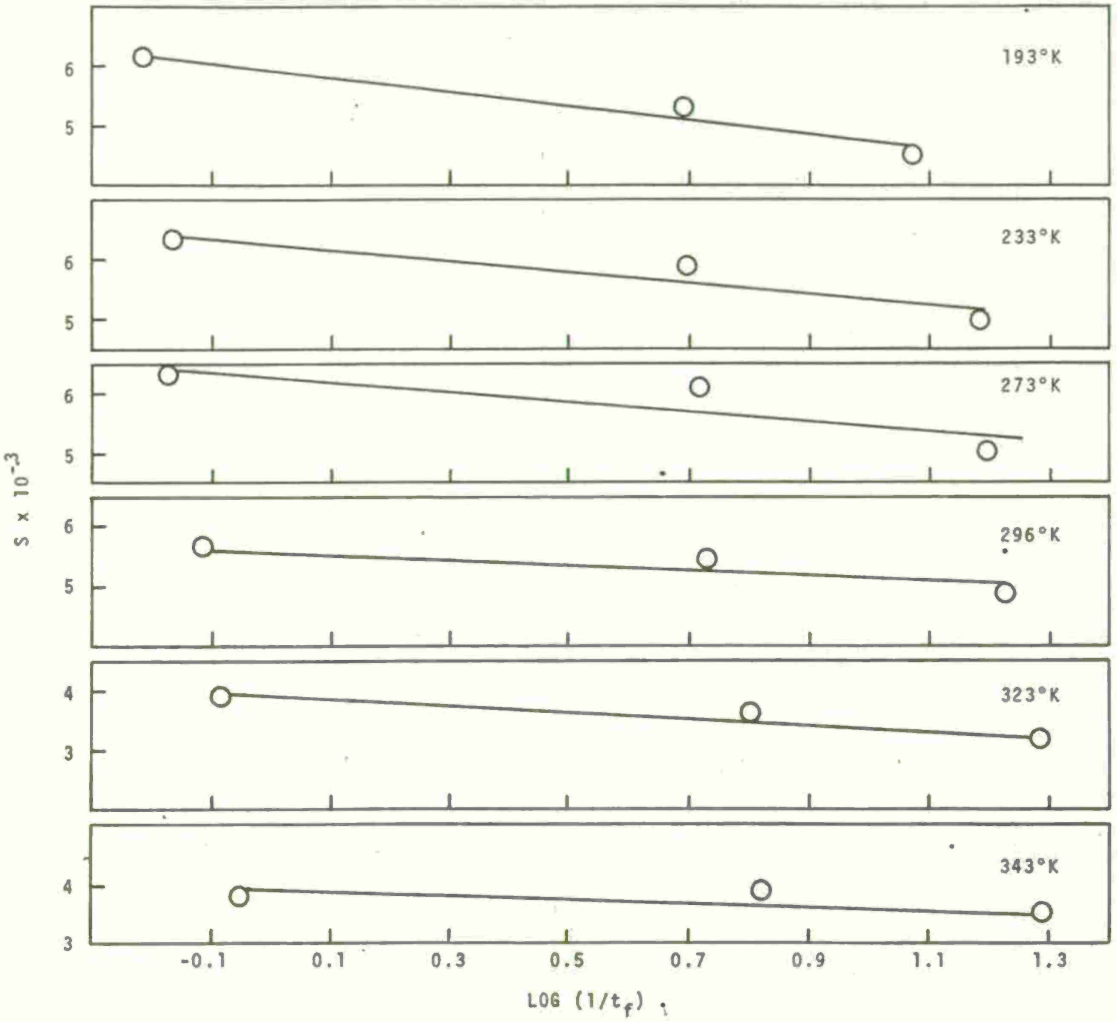

Fig 7 S versus log $(1/t_f)$ for AF126 adhesive with 1/8" aluminum adherends

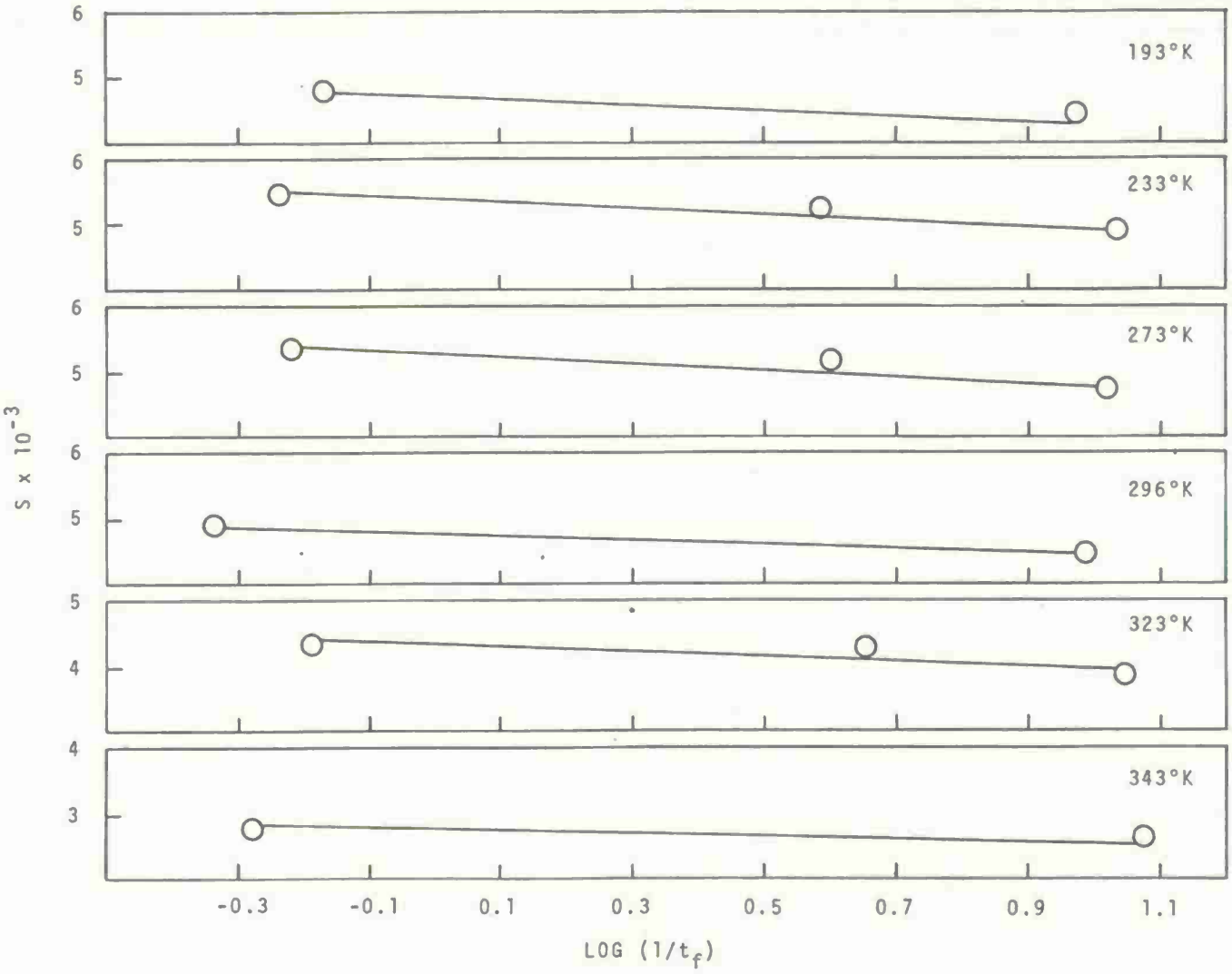

Fig 8 S versus log $(1/t_f)$ for AF126 adhesive with 1/16" aluminum adherends

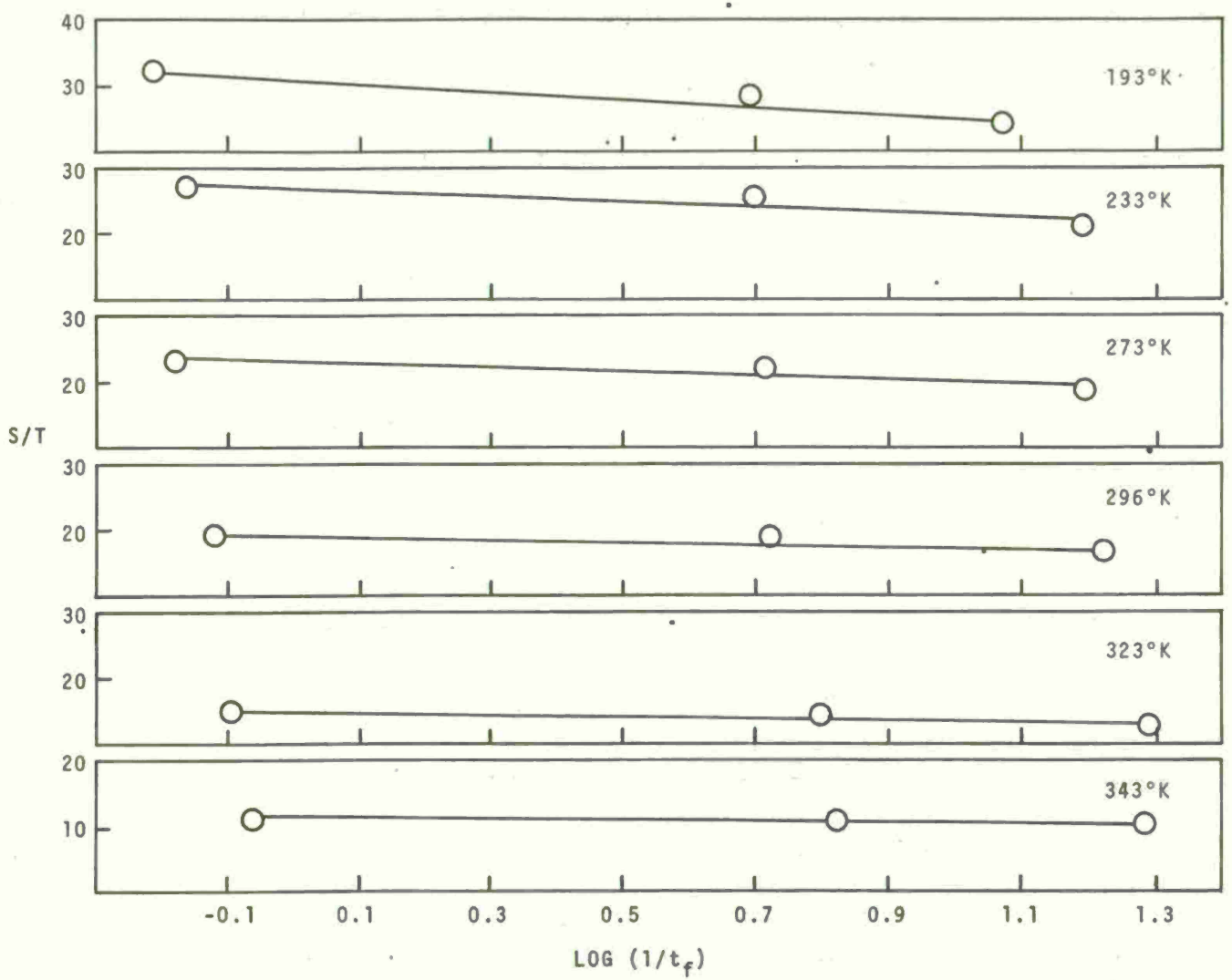

Fig 9 S/T versus log $(1/t_f)$ for AF126 adhesive with 1/8" aluminum adherends

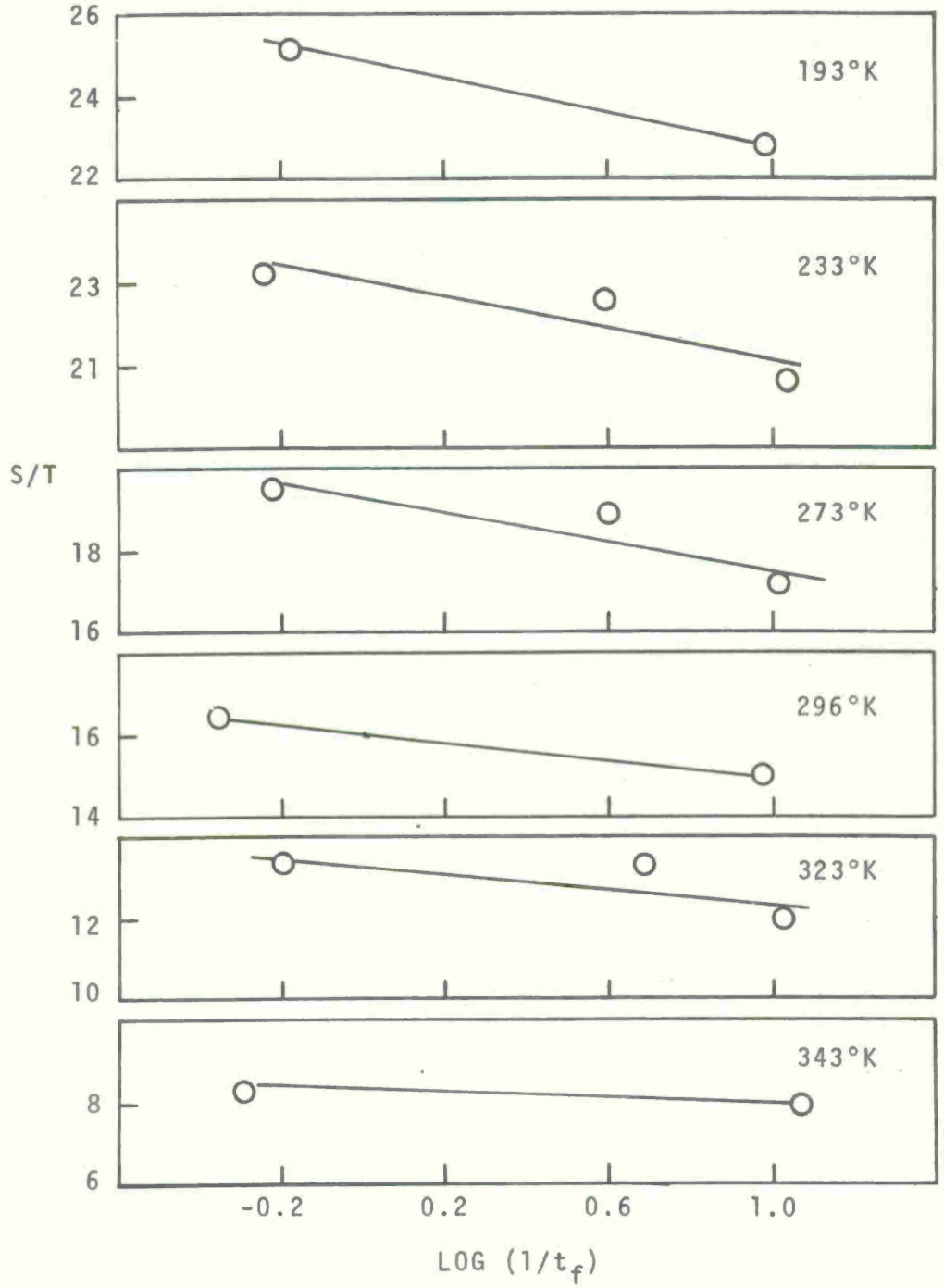

Fig 10 S/T versu log ($1/t_f$) for AF126 adhesive with 1/16" aluminum adherends

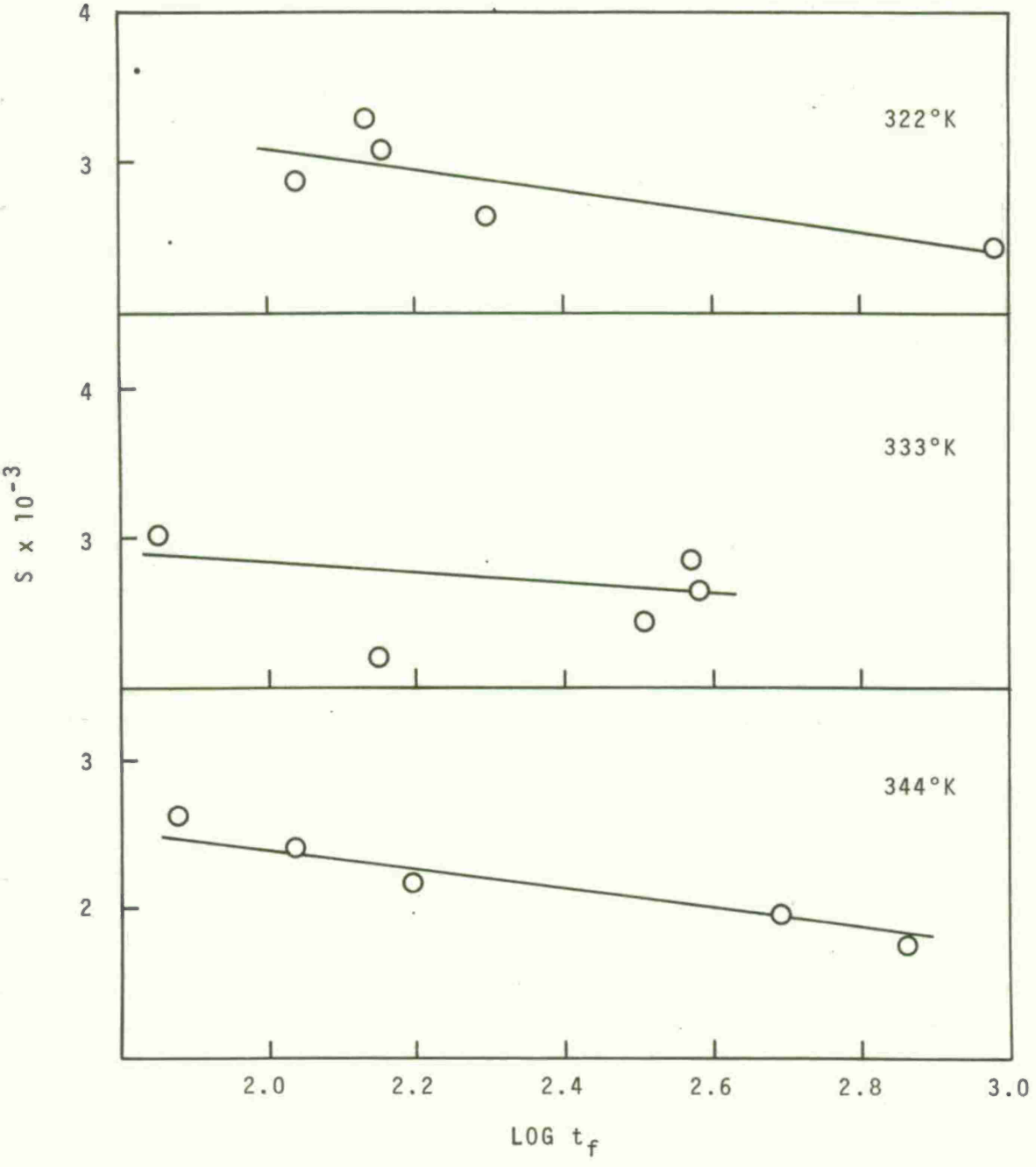

Fig 11 S versus log t_f for AF126 adhesive with 1/16" aluminum adherends 20% Relative humidity

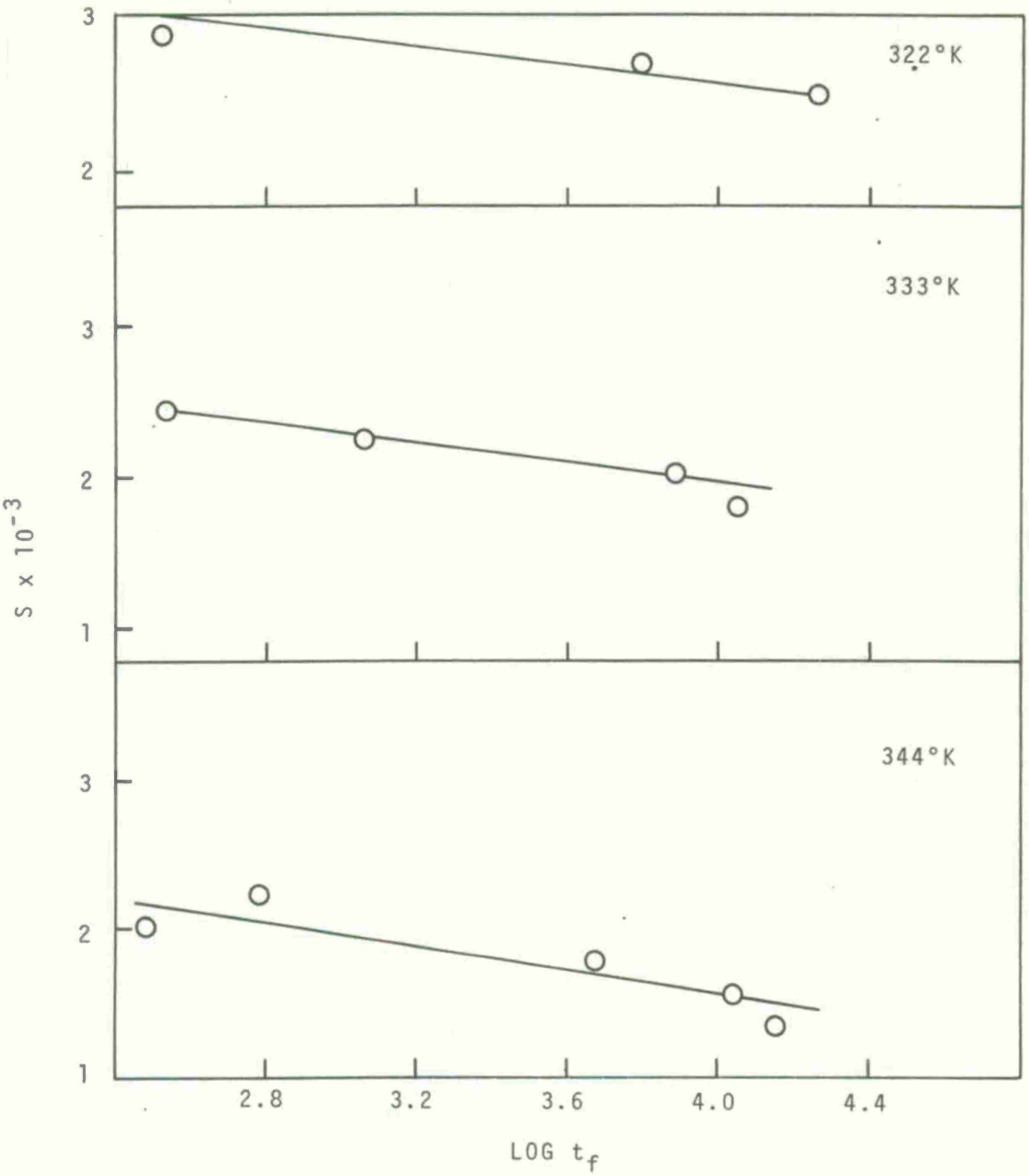

Fig 12 S versus log t_f for AF126 adhesive with 1/16" aluminum adherends 50% Relative humidity

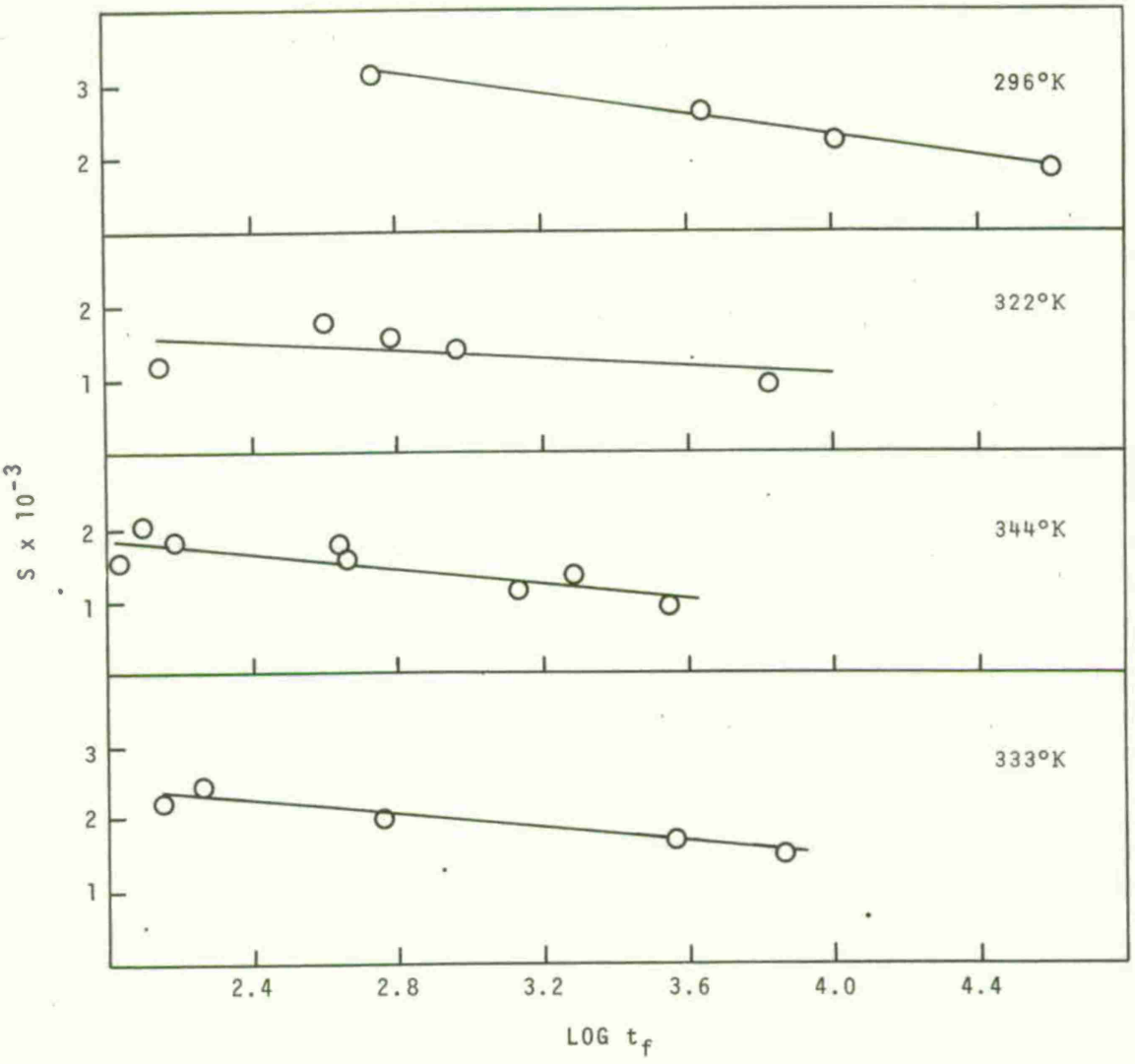

Fig 13 S versus log t_f for AF126 adhesive with 1/16" aluminum adherends 90-95% Relative humidity

DISTRIBUTION LIST

	Copy No.
Commanding Officer	
Picatinny Arsenal	
ATTN: Scientific and Technical Information Branch	1-6
SMUPA-VP6	7-23
SMUPA-T	24-28
SMUPA-D	29-33
SMUPA-N	34-35
SMUPA-I	36-37
SMUPA-ND	38
SMUPA-NR	39
Dover, New Jersey 07801	
Commanding General	
U. S. Army Materiel Command	
ATTN: AMCRD-T, Dr. H. M. El-Bisi	40
AMCRD-T, Mr. J. Rivkin	41
AMCPP-PI	42
AMC-QA	43
Physics and Electronics Br., Mr. John Beebe	44
Commanding General	
U. S. Army Missile Command	
ATTN: AMSMI-IE, Mr. J. E. Kirshstein	45
AMSMI-IEP, Mr. Giles Wetherill	46
AMSMI-RF, Dr. Julian S. Kobler	47
AMSMI-RH, Mr. Gregory S. Moshkoff	48
AMSMI-RL, Mr. William C. Watson	49
AMSMI-RTF, Mr. James M. Taylor	50
AMSMI-RSM, Mr. E. A. Verchot	51
AMSMI-RGP, Mr. Kenneth W. Plunkett	52
AMSMI-IELC, Mr. William B. Greene	53
AMSMI-IELC, Mr. Robert B. Clem	54
AMSMI-IELM-S, Mr. James R. Martin	55
AMSMI-RKK, Mr. C. H. Martin	56
Chief, Document Section	57
Redstone Arsenal, Alabama 35809	

Commanding General
U. S. Army Munitions Command
ATTN: AMSMU-RE-E, Mr. E. P. Burke 58
AMSMU-RE-E, Mr. W. G. McDaniel 59
AMSMU-RE-R, Mr. G. Chesnov 60
AMSMU-QA 61
AMSMU-CE, Chief Engineer 62
Dover, New Jersey 07801

Commanding General
U. S. Army Electronics Command
ATTN: AMSEL-PP/P/IED.2, Mr. Wes Karg 63
225 South 18th Street
Philadelphia, Pennsylvania 19103

Commanding General
U. S. Army Aviation Systems Command
ATTN: AMSAV-PRL, Mr. John Thorp 64
AMSAV-PPl, Mr. F. Matthews 65
AMSAV-EAA, Mr. R. Rodman 66
AMSAV-R-R(RD), Mr. R. Martin 67
AMSAV-EAC, Mr. J. Bramlet 68
AMSAV-R-R(RD), Mr. W. H. Brabson, Jr. 69
AMSAV-EAS, Mr. R. Reeves 70
AMSAV-EGSM, Mr. A. Taplits 71
AMSAV-R-R(RD), Dr. I. Peterson 72
P.O. Box 209, Main Office
St. Louis, Missouri 63166

Commanding General
U. S. Army Mobility Equipment Command
ATTN: AMSME-PLA, Mr. J. J. Murphy 73
AMSME-PLA, Mr. M. W. Schriet 74
4300 Goodfellow Blvd.
St. Louis, Missouri 63120

Commanding General
U. S. Army Tank-Automotive Command
ATTN: AMSTA-RCM.1, Mr. Don Phelps 75
AMSTA-RCM.1, Mr. Edward Moritz 76
Lt. Colonel John W. Wiss 77
Mr. Charles Green 78
Mr. Melvin A. Arvik 79
Warren, Michigan 48090

Commanding Officer
U. S. Army Materials and Mechanics Research Center
ATTN: AMXMR-TX, Mr. Arthur Jones 80
AMXMR-TX, Mr. P. A. Carbonaro 81
AMXMR-RF, Dr. G. Thomas 82
AMXMR-E, Mr. E. Hegge 83
AMXMR-QA 84
Technical Information Section 85
Watertown, Massachusetts 02172

Commanding Officer
Savanna Army Depot
ATTN: AMXSV-EN 86
AMC Ammunition Center
Savanna, Illinois 61704

Commanding Officer
Fort Detrick
ATTN: SMJFD, Mr. H. H. Meier 87
MD Division, Mr. D. E. Jones 88
MO Branch, Mr. H. Ralph Cunningham 89
Frederick, Maryland 21701

Commanding Officer
Rock Island Arsenal
ATTN: SWERI-PPE-5311, Mr. J. A. Fox 90
AMSWE-PPR, Mr. J. X. Walter 91
AMSWE-PPR, Mr. G. Hall 92
Rock Island Arsenal, Illinois 61201

Director
U. S. Army Production Equipment Agency
Rock Island Arsenal
ATTN: AMXPE-MT, Mr. H. Holmes 93-94
Rock Island Arsenal, Illinois 61201

Commanding Officer
U. S. Army Aeronautical Depot Maintenance Center
ATTN: SAVAE-EFT, Mr. J. A. Dugan 95
Corpus Christi, Texas 78419

Project Manager, General Purpose Vehicles
Michigan Army Missile Plant
ATTN: AMCPM-GPV-QV, Mr. E. A. Cowgill 96
AMCPM-GPV-T, Mr. L. F. Mortenson 97
Warren, Michigan 48090

Commanding Officer
U. S. Army Weapons Command
Watervliet Arsenal
ATTN: SMEWV-PPP-WP, Mr. L. Slawsky 98
Dr. Fred Schmiedeshoff 99
Dr. Robert E. Weigle 100
Dr. F. Sautter 101
Mr. W. G. McEwan 102
Mr. P. Rummel 103
Dr. Igbal Ahmad 104
Watervliet, New York 12189

Commanding General
U. S. Army Limited War Laboratory
ATTN: CRD-AM-6D 105
CRD-AM-7A, Mr. Hugh T. Reilly 106
CRD-AM-6C, Mr. Benjamin F. Wood, Jr. 107
CRD-AM-6C, Mr. R. P. McGowan 108
Aberdeen Proving Ground, Maryland 21005

Commanding Officer
Aberdeen Proving Ground
ATTN: Technical Library, Bldg 313 109
Aberdeen Proving Ground, Maryland 21005

Commanding Officer
Harry Diamond Laboratories
ATTN: Mr. A. A. Benderly 110
Library 111
Washington, D. C. 20438

Commanding General
U. S. Army Natick Laboratories
ATTN: Mr. Theodore L. Bailey 112
Dr. George E. Murray 113
Mr. Jack Furrer 114
Dr. J. Alden Murray 115
Natick, Massachusetts 01760

Commanding General
U. S. Army Electronics Command
ATTN: Mr. J. Spergel 116
Mr. D. A. Diebold 117
Mr. G. Plateau 118
Fort Monmouth, New Jersey 07703

Commanding Officer
U. S. Army Engineer Research and Development Labs
ATTN: Dr. George W. Howard 119
Mr. C. B. Griffis 120
Mr. H. Johnston 121
Mr. E. York 122
Mr. E. B. Holley 123
Fort Belvoir, Virginia 22060

Commanding Officer
U. S. Army Edgewood Arsenal
ATTN: Technical Information Branch 124
Mr. M. A. Raun, SMUEA-DME 125
Mr. N. Potash, SMUEA-DME-4 126
Mr. M. N. Timbs, SMUEA-QAEQ 127
Mr. B. Rogge, SMUEA-WCP 128
Edgewood Arsenal, Maryland 21010

Commanding Officer
Frankford Arsenal
ATTN: Dr. H. Gisser 129
Mr. M. Petronio 130
SMUPA-Q1000 131
Mr. H. Marcus 132
Mr. E. Kelly 133
Philadelphia, Pennsylvania 19137

Commanding Officer
Tobyhanna Army Depot
ATTN: Mr. N. J. DeMars 134
Mr. J. W. Tarrent 135
Tobyhanna, Pennsylvania 18466

Commanding Officer
U. S. Army Engineer Waterways Experiment Station
Corps of Engineers
ATTN: Mr. Robert Turner 136
Vicksburg, Mississippi 39180

Commanding General
U. S. Army Medical Biomechanical Research Laboratory
Water Reed Army Medical Center
ATTN: Dr. Fred Leonard 137
Forest Glen Section
Washington, D. C. 20012

Commanding General
U. S. Army Medical Equipment Research and
Development Laboratory
Fort Totten
ATTN: Mr. Donald O. Jones 138
Mr. Aaron Ismach 139
Flushing, Long Island, New York 11359

Plastics Technical Evaluation Center
ATTN: Mr. H. Pebly 140
Picatinny Arsenal
Dover, New Jersey 07801

Commanding General
White Sands Missile Range
ATTN: Technical Library 141
New Mexico 88002

Commanding Officer
Ammunition Procurement and Supply Agency
ATTN: AMUAP-QFO 142
Joliet, Illinois 60436

U. S. Naval Ordnance Laboratory
ATTN: Mr. F. R. Barnet 143
Silver Spring, Maryland 20910

Department of the Navy
Bureau of Naval Weapons
ATTN: RRMA, Airborne Equipment Division 144
Washington, D. C. 20360

Mr. D. M. McLeod, Supt. Materials Division
Naval Air Engineering Center
Building 76-5
Philadelphia, Pennsylvania 19112 145

Department of the Navy
Bureau of Naval Weapons
ATTN: RRMA-10 146
Washington, D. C. 20360

Naval Air Development Center
Aeronautical, Electronic and Electrical Laboratory
ATTN: Materials and Process Branch 147
Johnsville, Pennsylvania 18974

Naval Ship Research and Development Center
ATTN: Materials Research Branch 148
Washington, D. C. 20007

Defense Documentation Center
Cameron Station
Alexandria, Virginia 22314 — 149-159

U. S. Army Aviation Material Laboratory
ATTN: Mr. Roach — 160
Fort Eustis, Virginia 23604

Commander
Aeronautical Systems Division
ATTN: Mr. R. T. Schwartz — 161
Mr. R. C. Tomashot — 162
Mr. T. Reinhart — 163
Wright-Patterson Air Force Base, Ohio 45433

Commanding General
Headquarters, U. S. Air Force
Pentagon Building
Washington, D. C. 20330 — 164

National Aeronautics and Space Administration
Lewis Research Center
ATTN: Ch, Library — 165
21000 Brookpark Road
Cleveland, Ohio 44135

NASA Scientific and Technical Information Facility
Information Retrieval Branch
ATTN: Mr. William Neely — 166
P. O. Box 33
College Park, Maryland 20740

U. S. Army Research Office
ATTN: Dr. J. M. Majorwicz — 167
3045 Columbia Pike
Arlington, Virginia 22204

Director
U. S. Army Ballistics Research Laboratory
ATTN: Mr. Emerson V. Clarke, Jr. — 168
Dr. Eichelberger — 169
Mr. Herman P. Gay — 170
Aberdeen Proving Ground, Maryland 21005

Naval Underwater Weapons Station
Research Department
ATTN: Mr. F. Spicola 171
Newport, Rhode Island 02840

Naval Air Systems Command
Industrial Resources Branch
ATTN: Mr. P. Robinson 172
Washington, D. C. 20360

Naval Electronic Laboratory Center
ATTN: Mr. Harvey F. Dean, Code S-340 173
San Diego, California 92152

Naval Ordnance Systems Command
Industrial Resources Division
ATTN: Mr. T. E. Draschil, Code 0471E 174
Washington, D. C. 20360

U. S. Navy Ships Systems Command Hdqtrs.
ATTN: Mr. T. Kelley, Code 703A 175
Annapolis Academy
Annapolis, Md. 21402

Naval Research Laboratory
ATTN: Mr. W. Oaks, Code 2343 176
Washington, D. C. 20390

Naval Ordnance Station
ATTN: Mr. T. Peake 177
Southside Drive
Louisville, Ky. 40214

Naval Avionics Facility
ATTN: Mr. B. D. Togue, Code D/803 178
21st and Arlington
Indianapolis, Ind. 46218

Naval Material Industrial Resources Office
ATTN: Mr. L. F. Walton 179
Mr. H. Shapiro 180
Philadelphia, Pa. 19112

Commanding General
U. S. Army Materiel Command
ATTN: Mr. J. Dockins, AMCPM-UA-T 181
Mr. C. Cioffi, AMCPM-LH-T 182
P. O. Box 209
St. Louis, Mo. 63166

Headquarters
U. S. Air Force (AFRDDA)
Washington, D. C. 20330 183

Headquarters
Air Force Armament Laboratory (ATX)
Eglin Air Force Base, Florida 32542 184

Headquarters
Air Force Systems Command (SCTS)
Andrews Air Force Base, Md. 20331 185

Headquarters
Air Force Weapons Laboratory (WLX)
Kirtland Air Force Base, N. M. 87117 186

Deputy Commanding General
U. S. Army Munitions Command
ATTN: AMSMU-MM-B
Joliet, Illinois 60436 187

UNCLASSIFIED

Security Classification

DOCUMENT CONTROL DATA - R & D

(Security classification of title, body of abstract and indexing annotation must be entered when the overall report is classified)

1. ORIGINATING ACTIVITY (Corporate author)	2a. REPORT SECURITY CLASSIFICATION
Picatinny Arsenal, Dover, N. J.	UNCLASSIFIED
	2b. GROUP

3. REPORT TITLE

FAILURE OF ADHESIVE BONDS AT CONSTANT STRAIN RATES

4. DESCRIPTIVE NOTES (Type of report and inclusive dates)

5. AUTHOR(S) (First name, middle initial, last name)

Elise McAbee, Michale J. Bodnar, William C. Tanner and David W. Levi

6. REPORT DATE	7a. TOTAL NO. OF PAGES	7b. NO. OF REFS
MARCH 1971	41	3

8a. CONTRACT OR GRANT NO.	9a. ORIGINATOR'S REPORT NUMBER(S)
b. PROJECT NO.	Technical Report 4152
c. AMCMS Code 4010.28.9.02003	9b. OTHER REPORT NO(S) (Any other numbers that may be assigned this report)
d.	

10. DISTRIBUTION STATEMENT

Approved for public release; distribution unlimited.

11. SUPPLEMENTARY NOTES	12. SPONSORING MILITARY ACTIVITY

13. ABSTRACT

Shear strengths of adhesive AF126 bonds to two thicknesses of aluminum were measured at constant rate of crosshead separation. Primarily cohesive failure was observed in all cases. By using relations proposed by Cherry and Holmes, the shear strength could be quantitatively related to temperature and strain rate or failure time. Of specific engineering interest would be the possibility of determining the reliability of a bonded joint for specific periods of time as a function of continuously applied stress at a given temperature.

DD FORM 1 NOV 68 1473 REPLACES DD FORM 1473, 1 JAN 64, WHICH IS OBSOLETE FOR ARMY USE.

UNCLASSIFIED

Security Classification

14. KEY WORDS	LINK A		LINK B		LINK C	
	ROLE	WT	ROLE	WT	ROLE	WT
Adhesive bonds, failure of						
Constant strain rates						
AF126 adhesive						
Aluminum (2024-T3) adherends, 1/8 inch						
Aluminum (2024-T3) adherends, 1/16 inch						
Lap shear specimens						
Temperature effects (193°, 233°, 273°, 296°, 323°, 343°K)						
RH effects (20%, 50%, 90-95%)						
Shear strength of structural adhesives						
Deformation of adherends						
Preparation of adherends						
Preparation of specimens						
Test procedures						